

Sampling of Shifted Fan Beam Projections for Region of Interest Reconstruction

Jeffrey Brokish^{1,2} and Yoram Bresler²

¹InstaRecon, Inc., Urbana, Illinois, USA

²Coordinated Science Lab and Dept. ECE,

University of Illinois at Urbana-Champaign, Urbana, Illinois, USA

Abstract—The sampling requirements in fan-beam tomography are well known and provide an estimate of the number of projections required for accurate reconstruction of the entire image. Here we consider the problem of reconstructing a small, off-center subregion of the object. We show that a subregion can be reconstructed from a smaller set of projections, reducing the computation required to form the image. The analysis requires the study of the essential support of the Fourier transform of shifted fan beam projections, which have not previously been analyzed.

I. INTRODUCTION

The sampling requirements of fan-beam projection data have been previously studied [1] and determine the number of projections necessary for accurate reconstruction of the *entire* image. Here we restrict the reconstruction region to a small, off-center subregion of the object. This arises in hierarchical backprojection [2], where the image is subdivided into non-overlapping subregions, which are reconstructed independently and merged to form the final image. The problem also arises when only a small region of interest is to be reconstructed. We show that a subregion can be accurately recovered from a smaller set of projections, which reduces the amount computation required in the reconstruction.

II. PRELIMINARIES

Consider the fan beam geometry with an equiangular detector shown in Figure 1, with an x-ray source rotating on a circle of radius D about an object of radius R , producing fan beam projection data $g(\alpha, \beta)$ at source angle β and fan angle α . Define the fan angle of point ξ from source position β as the function $\alpha_\xi(\beta)$. The following analysis can be adapted for the case of a flat detector array by substituting the appropriate function for $\alpha_\xi(\beta)$.

The sampling requirements of $g(\alpha, \beta)$ are determined by its spectral support. Since $g(\alpha, \beta)$ is periodic in both α and β , the bandwidth analysis computes the 2-D Fourier series coefficients for integer values m and k .

$$G(m, k) = \int_{-\pi}^{\pi} \int_{-\pi/2}^{\pi/2} g(\alpha, \beta) e^{j(m\alpha + k\beta)} d\alpha d\beta \quad (1)$$

This material is based upon work supported under a National Science Foundation Graduate Research Fellowship and by NSF grants Nos. CCR 99-72980 and CCR 02-09203.

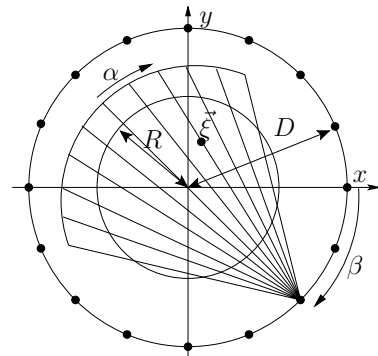


Fig. 1. Fan Beam Scanning

Since the object is spatially limited and usually has non-smooth radially asymmetric parts, $G(m, k)$ will not be strictly band-limited in either m or k . Therefore, for fixed m , the angular bandwidth analysis involves finding the *essential support* of (1), which is defined as the region outside which the function decays exponentially. Previous analyses [1] of $G(m, k)$ indicate that the region of essential support has a tilted bowtie shape, which is a function of the size of the object and the geometry of the scan. In particular, the width of the bowtie in the angular frequency variable k is proportional to the radius of the bounding circle of the object.

III. PROBLEM DESCRIPTION

The objective is to reconstruct a small, circular region of interest (ROI) of radius r offset from the origin a distance c , as shown in Figure 2. Analysis of the sampling requirements [1] that relies on the essential support of (1) provides the number of projections required to reconstruct the entire object. However, this overestimates the projections needed to reconstruct only the ROI.

The reconstruction of a smaller, origin-centered ROI of radius r only requires data corresponding to the smaller bowtie support of that smaller region. This is the case when the number of projections is large enough to prevent the bowtie support of the full object from aliasing into this region. In addition, the projections can then be decimated (i.e. angularly lowpass filtered and downsampled) to a set of size equivalent

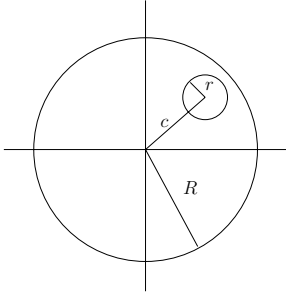


Fig. 2. ROI Reconstruction

to the width of the ROI's spectral bowtie. This reduces the computational effort required in the reconstruction of this ROI.

When the ROI is off-centered, as in Figure 2, then its bowtie spectral support equals that of an origin-centered region of radius $r + c$, which will not provide appreciable savings for a ROI far from the origin. A "re-centering" technique used in hierarchical backprojection for fan beam data [3] involves shifting each projection relative to the projection $\alpha_c(\beta)$ of the subregion center. As shown in Figure 3, this shift reduces the angular bandwidth of the ROI's spectral bowtie, which allows for a much larger decimation ratio of the projection data. This analysis examines the spectral support of shifted fan beam projections and provides the new angular sampling requirements of the shifted projection data.

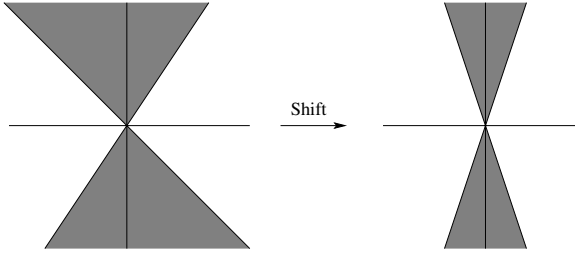


Fig. 3. ROI Bowtie Before and After Shifting

IV. BANDWIDTH OF SHIFTED FAN BEAM PROJECTIONS

The shifted projection data is expressed as $\hat{g} = g(\alpha + \alpha_c(\beta), \beta)$. The Fourier integral of (1) becomes

$$\hat{G}(m, k) = \int_{\pi}^{\pi} \int_{-\pi/2}^{\pi/2} g(\alpha + \alpha_c(\beta), \beta) e^{j(m\alpha + k\beta)} d\alpha d\beta \quad (2)$$

The interplay between the α and β coordinates prevents analysis of (2) using previously established methods [1], which were able to separate the double integral and evaluate an inner integral. This analysis addresses this issue by considering the contributions of each point in the ROI to the essential support of shifted projections $\hat{G}(m, k)$. This essential support will be the union of the spectral support for all such points.

Define a point in the ROI as \vec{u} . The fan beam projections of this point can be expressed (with a shift) as

$$\hat{g}_u(\alpha, \beta) = \delta(\alpha - \alpha_u(\beta) + \alpha_c(\beta), \beta) \quad (3)$$

Fan-beam projections of a δ also involve a weighting that is a function of β . This has been omitted from (3) as it has been shown [4] that it does not have a meaningful contribution to the essential support of $\hat{G}(m, k)$.

Substituting (3) into (2) allows the evaluation of the α integral, yielding

$$\hat{G}_u(m, k) = \int_0^{2\pi} e^{j(m[\alpha_c(\beta) - \alpha_u(\beta)] + k\beta)} d\beta \quad (4)$$

Let $\epsilon(\beta) = \alpha_c(\beta) - \alpha_u(\beta)$. This function is periodic in β and can be written in the polar form of its Fourier series expansion

$$\epsilon(\beta) = \sum_{n=1}^{\infty} a_n \sin(n\beta + \phi_n) \quad (5)$$

Substituting this expansion into (4) results in the Fourier series coefficients in β of a product of exponentials. This is equivalent to the convolution in k of the Fourier series coefficients of each term

$$\hat{G}_u(m, k) = \hat{G}_u^1(m, k) \star_k \hat{G}_u^2(m, k) \star_k \hat{G}_u^3(m, k) \dots \quad (6)$$

The n th term in the convolution is

$$\hat{G}_u^n(m, k) = e^{-k\phi_n/n} \int_0^{2\pi} e^{j(m a_n \sin(n\beta) + k\beta)} d\beta \quad (7)$$

The results obtained here rely on the properties of the Bessel function of the first kind, which is defined

$$J_k(m) = \int_{-\pi}^{\pi} e^{j(m \sin(x) + kx)} dx \quad (8)$$

Examination of the properties of $J_k(m)$ shows that it decays exponentially with m when $|k| > |m|$. A modified form that appears in (7) is

$$J_{k \uparrow n}(m) = \int_{-\pi}^{\pi} e^{j(m \sin(nx) + kx)} dx \quad (9)$$

for n an integer. It has been demonstrated [4] that $J_{k \uparrow n}(m)$ decays exponentially with m for $|k| > |nm|$.

For fixed m , the width in k of the essential support of the convolution is bounded by the sum of the essential support width for each term in the convolution. The complex phase factor in (7) does not modify the essential support of G^n , which will have width $n|a_n m|$ according to (9). Therefore, the bandwidth of the projections of the shifted point can be expressed as

$$B\{\hat{G}_u\}(m) \leq |m| \sum_{n=1}^{\infty} n|a_n|. \quad (10)$$

Notice that this function is linear in m , indicating that the support retains its bowtie structure. A less conservative boundary can be determined by incorporating the phase terms dropped from (7). Convolution of all n terms is difficult to determine analytically, so instead the convolution of the first two terms can be calculated numerically. The width of the essential support of this convolution is a function that can be precalculated and tabulated. The contribution of remaining terms can be estimated conservatively using the previous method.

The essential support estimate using (10) or the less conservative method defines a region that is described by two straight lines. The essential support corresponds to all k that satisfy

$$\begin{aligned} k &\in [-\gamma_L(\vec{u})m, \gamma_R(\vec{u})m] & m \geq 0 \\ k &\in [\gamma_R(\vec{u})m, -\gamma_L(\vec{u})m] & m < 0 \end{aligned} \quad (11)$$

The bandwidth estimate of (10) yields a symmetric estimate in k with $\gamma_L = \gamma_R$. The less conservative method, however, will provide an asymmetric region. Figure 5 in the simulations section demonstrates the difference between these two estimates.

The essential support of projections of an entire region Ξ is bounded by the union of the essential support of the projections of each point inside that region. This support is also bowtie shaped, which can be described as

$$\begin{aligned} \gamma_L(\Xi) &= \max_{\vec{u} \in \Xi} \gamma_L(\vec{u}) \\ \gamma_R(\Xi) &= \max_{\vec{u} \in \Xi} \gamma_R(\vec{u}) \end{aligned} \quad (12)$$

This bowtie will contain the essential support of all points that lie inside the region.

Based on this bandwidth estimate, it is possible to estimate the sampling requirements for reconstructing the ROI. The initial number of projections collected must be sufficient to avoid aliasing of the bowtie support of the full object onto the bowtie support of the ROI. Let Ξ correspond to the spatial support of the full object and Λ correspond to the spatial support of the ROI. Aliasing will be avoided when the number of projections satisfies

$$P_{min} = \bar{m} \max(\gamma_R(\Lambda) + \gamma_L(\Xi), \gamma_L(\Lambda) + \gamma_R(\Xi)) \quad (13)$$

where \bar{m} is the maximum frequency content along the fan angle coordinate over all projections. This condition is shown in Figure 4, with the dark bowtie indicating the spectral support of the ROI after shifting and the light bowtie indicating the spectral support of the full object after shifting. This is the tightest packing in k of the two bowties that prevents aliased copies of the full object bowtie from overlapping the ROI bowtie. As long as the number of projections collected

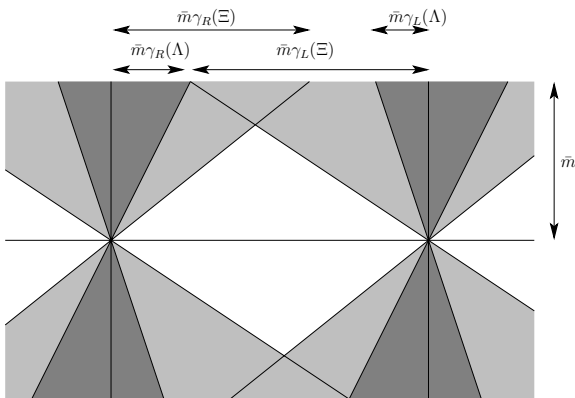


Fig. 4. Minimum angular sampling condition

exceeds this minimum, the projections can be shifted and then

decimated in source angle. The decimation filter truncates the bowtie supports in angular frequency at $k = \pm \bar{k}$ for

$$\bar{k} = \bar{m} \max(\gamma_R(\Lambda), \gamma_L(\Lambda)) \quad (14)$$

which is maximum width of the ROI bowtie after shifting. This retains all the contributions of the ROI, and rejects all out-of-band contributions of points outside the ROI. The projections can then be downsampled without aliasing to the minimum projection count $\bar{P}_{min} = 2\bar{k}$.

V. COMPUTATIONAL SAVINGS

The computational bottleneck in image reconstruction using filtered backprojection (FBP) is the weighted backprojection of filtered projection data, which requires computationally expensive geometric calculations (including divisions and arc-tangents) and has overall complexity of $O(N^2P)$.

When the projection data can be successfully decimated to \bar{P} projections, then the cost of backprojection is reduced by \bar{P}/P . The decimation operation is performed by first shifting the data and then decimating in source angle. The filtering operation in the FBP is typically performed in the frequency domain. In this case the shifting operation can be combined with the filtering operation at negligible overhead. The angular decimation can be performed exactly using the FFT, but the cost of this operation may offset the savings gained in the reduction of the backprojection cost. Instead, this decimation operation can be performed using a short filter in the spatial domain if the decimation factor chosen is a ratio of integers. In this case the decimation operation has complexity $O(NP)$, which has a negligible contribution to the overall computation in reconstructing the ROI.

VI. SIMULATIONS

Figure 5 compares a numerical evaluation of bow-tie support in (4) to the bandwidth estimates derived from (10). The two cases shown are $\vec{u} = [64, 0]$, $c = [0, 0]$ (left column) and $\vec{u} = [64, 0]$, $c = [96, 0]$ (right column). Estimates using the conservative bound are denoted by solid lines, with the less conservative bound shown with dashed lines. The horizontal dotted line is the cut shown in the plot below each bowtie on a log scale, demonstrating the exponential decay outside the bowtie region.

A ROI example is shown in Figure 6 for a phantom consisting of disks of varying radii and constant value 1. The ROI is denoted by a dashed circle (not part of the phantom). Applying the above analysis indicates that the full object would require 2550 projections, while reconstruction of the ROI requires an initial set of 2340 projections, which can then be decimated to 694 projections. This decimation can be achieved using the FFT, or a slightly larger set of 780 projections can be formed that involves decimation by a factor of 3. This enables the use of short decimation kernels leading to a very inexpensive decimation operation. In this case a length 9 lowpass filter designed for cutoff $\pi/3$ was used as the angular decimation filter when forming a set of 780 projections. The reconstruction

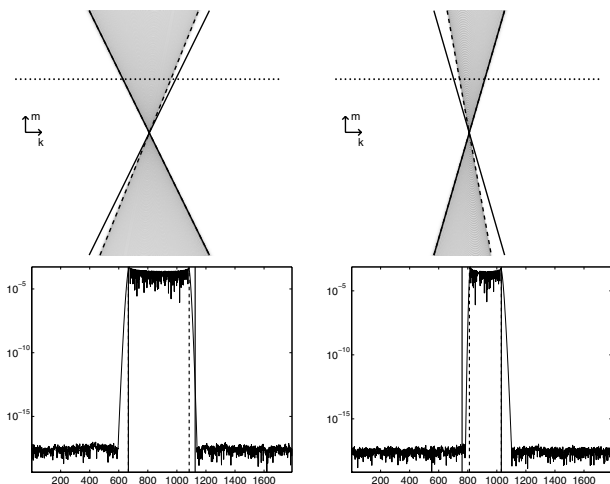


Fig. 5. Bowtie support for $x = [64, 0]$, $c = [0, 0]$ (left column) and $x = [64, 0]$, $c = [96, 0]$ (right column)

from this decimated set is shown in Figure 7A. The absolute difference between the reconstructions with full and decimated data over the entire image is shown in Figure 7B on a scale $[0 \ 0.01]$. The ROI falls within the region of negligible error. The peak difference inside the ROI is $4 \cdot 10^{-3}$. This peak error is reduced by about 10% by using the FFT to perform the decimation. The use of the inexpensive decimation filter results in a computational ratio of 3.3 versus reconstruction of the ROI directly from the full object projection data.

VII. CONCLUSION

The study of sampling conditions for fan beam projection data is important for keeping the computation required for image formation to a minimum. In this paper we examined the essential support of shifted fan beam projection data and demonstrated how it can be used to reconstruct a ROI with a decimated projection set. This analysis will also be important in providing a justification of hierarchical reconstruction algorithms for fan beam geometries.

REFERENCES

- [1] F. Natterer, Sampling in Fan Beam Tomography. *SIAM Journal Applied Mathematics*, pp. 358-380, 1993.
- [2] S. Basu and Y. Bresler, An $O(N^2 \log N)$ Filtered Backprojection Reconstruction Algorithm for Tomography. *IEEE Transactions on Image Processing*, pp. 1760-1773, 2000.
- [3] S. Xiao, Y. Bresler, and D. Munson, $O(N^2 \log N)$ Native Fan-Beam Tomographic Reconstruction, *Proceedings of the 1st IEEE International Symposium on Biomedical Imaging*, pp. 824-827, 2002.
- [4] J. Brokish, Fast Backprojection Algorithms for Divergent Beam Tomography, Ph.D. Dissertation, University of Illinois at Urbana-Champaign, 2004.

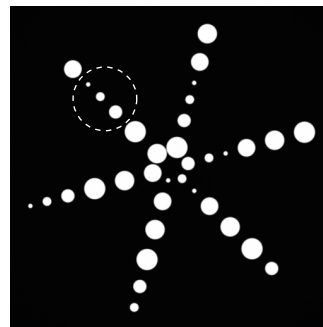


Fig. 6. Phantom and ROI (dashed circle)

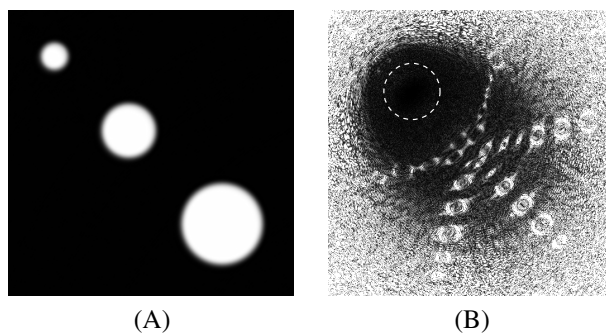


Fig. 7. (A) ROI reconstruction from decimated projections and (B) Error between full and decimated projection reconstructions